第49卷第4期 中国科学技术大学学报 Vol. 49, No. 4
2019年4月 JOURNAL OF UNIVERSITY OF SCIENCE AND TECHNOLOGY OF CHINA Apr. 2019

文章编号:0253-2778(2019)04-0259-09

Improved electrochemical reversibility of Li-Ni-Te-O cathode by local domain structure optimization

QI Jiaxin[1], WANG Xingbo[1], SU Xiaozhi[2], XIE Hui[1], REHMAN Zia ur[1], TAO Shi[3], CHU Wangsheng[1]

(1. *National Synchrotron Radiation Laboratory, University of Science and Technology of China, Hefei* 230029, *China*;
2. *Shanghai Synchrotron Radiation Facility, Shanghai Institute of Applied Physics, Chinese Academy of Sciences, Shanghai* 201204, *China*;
3. *Department of Physics and Electronic Engineering, Changshu Institute of Technology, Changshu* 215500, *China*)

Abstract: Novel layered oxide $Li_{1+x}Ni_{3/4-5/4x}Te_{1/4+1/4x}O_2$ ($x=0$, 0.14, 0.33, 0.46, 0.50 and 0.60) cathodes were synthesized by a solid-state reaction method. A unique $P\bar{1}$-like domain with a short-range order around Ni ions was found in the monoclinic $C2/m$ crystal with $x=0.33$, which displays a loosely bonded local structure and increased Li^+ mobility, enabling superior structural as well as electrochemical reversibility. The enhanced properties investigated by *ex situ* X-ray absorption spectroscopy (XAS), X-ray diffraction (XRD), X-ray photoelectron spectroscopy (XPS) and electrochemical characterization were corroborated to originate from the stable short- and long-range ordering structure along with the Ni electron redox. This study may open up new avenues for the development of Li-rich cathode materials with sufficiently good performance.

Key words: Li-ion battery; cathode material; local structure

CLC number: O646.21 **Document code**: A doi:10.3969/j.issn.0253-2778.2019.04.001

Citation: QI Jiaxin, WANG Xingbo, SU Xiaozhi, et al. Improved electrochemical reversibility of Li-Ni-Te-O cathode by local domain structure optimization[J]. Journal of University of Science and Technology of China, 2019,49(4):259-267.
齐家新,王星博,苏晓智,等. 局域结构优化 Li-Ni-Te-O 正极的电化学可逆性[J]. 中国科学技术大学学报,2019,49(4):259-267.

局域结构优化 Li-Ni-Te-O 正极的电化学可逆性

齐家新[1],王星博[1],苏晓智[2],解 晖[1],REHMAN Zia ur[1],陶 石[3],储旺盛[1]

(1. 中国科学技术大学国家同步辐射实验室,安徽合肥 230026;2. 中国科学院上海应用物理研究所上海光源,上海 201204;
3. 常熟理工学院物理与电子工程学院,江苏常熟 215500)

摘要: 利用固相法合成了一系列化合物 $Li_{1+x}Ni_{3/4-5/4x}Te_{1/4+1/4x}O_2$($x=0$, 0.14, 0.33, 0.46, 0.50 和 0.60). 在 $x=0.33$ 时,发现 $C2/m$ 晶体结构中存在一种新奇的围绕 Ni 离子的短程有序 $P\bar{1}$-like 区域,此区域表现出一种松散结合的局域结构以及更快的 Li^+ 迁移率,进而保证了优越的结构和电化学可逆性. 通过非原位 X 射线吸收谱(XAS)、X 射线衍射(XRD)、X 射线光电子能谱(XPS)和电化学表征研究了材料的性能. 证明了这

Received: 2018-03-01; **Revised**: 2018-05-22

Foundation item: Supported by the National Natural Science Foundation of China (11275227, U1632103).

Biography: QI Jiaxin, male, born in 1991, master. Research field: energy storage and conversion material. E-mail: qjiaxin@mail.ustc.edu.cn

Corresponding author: CHU Wangsheng, PhD/Prof. E-mail: chuws@ustc.edu.cn

种性能与稳定的短程-长程有序结构以及 Ni 氧化还原电子对有关. 该研究提供了发展高性能富锂正极材料的新思路.

关键词: 锂离子电池;正极材料;局域结构

0 Introduction

Secondary lithium-ion batteries as an alternative energy storage system are widely used in various electronic applications, such as stationary energy storage, smart grid and electronic vehicles[1-4]. Layered oxides such as α-$NaFeO_2$/$LiCoO_2$ type structure have received widespread attention for their excellent electrochemical properties[5]. However, the rechargeable capacity of $LiCoO_2$ is limited to 160 mAh · g^{-1} due to the destruction of crystal structure[6-8]. Among these layered materials, Ni-containing cathodes can deliver high capacity and comparably high operating voltage at a lower cost[9], such as $LiNi_{0.5}Mn_{0.5}O_2$[10-11] and lithium nickel manganese cobalt oxide (NCM)[12] layered cathode material with an increased capacity of more than 200 mAh · g^{-1} because of the dual electron redox of Ni element. However, this does not mean a high content of Ni can bring about a satisfactory capacity. The high Ni content may lead to structural transition and surface instability, resulting in severe capacity decay during cycling[13-14]. For these reasons, Ni is often used as a dopant in the electrode material to enhance the electrochemical performance[15-16].

Recently, a range of cations with high valence were introduced to form high lithium containing oxides in order to gain high capacity, such as $LiNi_{0.67}Sb_{0.33}O_2$[17], Li_4MoO_5-NiO[18] and Li_3MRuO_5[19], that holds a significant potential as new host structures for high capacity cathode materials. Li_4TeO_5 is also classified as a layered structure[20]. However, it is electrochemically inactive owing to the absence of electrons in the conduction band of tellurium. Hence, transition metals[21-24] are partially substituted for Te^{6+} and Li^+ to induce electrical conductivity in Li_4TeO_5. Considering NiO crystallizes into the layered oxide similar to Li_4TeO_5, NiO-Li_4TeO_5 binary system can be structured with the possibility of potentially rich Li-content and stable Niredox.

As we all know, tellurium is much more expensive than nickel and therefore not suitable for use in large-scale battery cathodes. So the ultimate goal of our research is to find a strategy for increasing the content of low cost constituents (like Ni), and get excellent electrochemical performance at the same time. In this work, we introduced NiO into Li_4TeO_5 system in the form of aNiO · $b$$Li_4TeO_5$ (a : b = 3, 2, 1, 1/2, 1/3, 0) which can be simply rewritten as $Li_{1+x}Ni_{3/4-5/4x}Te_{1/4+1/4x}O_2$ (x = 0, 0.14, 0.33, 0.46, 0.50, 0.60) as a Li-excess electrode for convenience and found a unique $P\bar{1}$-like domain with a short-range order around Ni ions in a monoclinic $C2/m$ crystal, resulting in an improved Li^+ extraction and structural stability. The structure and electrochemical performance of Li-Ni-Te-O were systematically investigated in this study. This article will serve as a preliminary study for lithium ion battery used in large-scale applications and the efforts we have made will contribute to future research in this field.

1 Experimental

1.1 Materials preparation

$Li_{1+x}Ni_{3/4-5/4x}Te_{1/4+1/4x}O_2$ was synthesized by a simple solid-state reaction method[25]. Li_2CO_3, $NiC_4H_6O_4$ · $4H_2O$ and TeO_2 were prepared as precursors in desired ratios and an excess of 10% lithium is required to compensate for lithium loss during high temperature calcination. The precursors were mixed by planetary ball milling. Then, the mixtures were calcined at 1000 ℃ for 16 h in air. After cooling to room temperature, the powder was carefully ground followed by

heating at 1050 ℃ for 6 h.

1.2 Materials characterization

The results were characterized by powder X-ray diffraction (XRD, D8-Advance power diffractometer, CuKα radiation, λ=1.54178 Å). Ni and Te X-ray photoelectron spectra (XPS) were collected by a spectrometer (ESCALAB 250). Ni K-edge X-ray absorption structure (XAS) measurements were performed in transmission mode using 1W2B beamline at Beijing synchrotron radiation facility (BSRF). Data analysis was carried out using the IFEFFIT software.

1.3 Electrochemical measurements

Electrochemical behavior of $Li_{1+x}Ni_{3/4-5/4x}Te_{1/4+1/4x}O_2$ as a cathode material was tested in Li half CR2032 coin cells. Composite electrodes were prepared with the active material, acetylene carbon black and PVDF in a mass ratio of 8∶1∶1, and then rolled into a film. Coin-type cells (CR2023) were assembled in an argon-filled glove box (UniLab, Mbraun, Germany) using Li metal as counter electrode, Celgard 2400 as separator and 1 mol/L $LiPF_6$ in a mixture of ethylene carbonate and dimethyl carbonate (1∶1, volume ratio) as electrolyte. Galvanostatic charge/discharge tests were performed on a Land CT2001A (Wuhan, China) between 3.5 and 4.6 V vs. Li^+/Li. Electrochemical impedance spectroscopy (EIS) and cyclic voltammetry (CV) were measured on a CHI660D (Chenhua, Shanghai) electrochemical workstation.

2 Results and discussion

Fig. 1(a) shows the XRD patterns of the obtained $Li_{1+x}Ni_{3/4-5/4x}Te_{1/4+1/4x}O_2$ ($x=0$, 0.14, 0.33, 0.46, 0.50 and 0.60). The samples $LiNi_{0.75}Te_{0.25}O_2$ ($x=0$), $Li_{1.14}Ni_{0.58}Te_{0.28}O_2$ ($x=0.14$) and $Li_{1.33}Ni_{0.33}Te_{0.33}O_2$ ($x=0.33$) can be classified as layered structure in a space group of $C2/m$ (PDF # 00-58-638). These three samples exhibit noticeable superlattice peaks within a 20°～23°range, suggesting a high stacking order of the transition metal layer along the c axis[26]. The as-prepared Li_4TeO_6 ($x=0.60$) is indexed to space group $P\bar{1}$ (PDF # 84-1362). Part of the peaks of $Li_{1.46}Ni_{0.18}Te_{0.36}O_2$ ($x=0.46$) can be indexed based on $C2/m$ structure except for the unconventional peaks at about 19°～44° (arrows), which can be indexed to $P\bar{1}$ structure. It indicates that the samples were gradually transformed into $P\bar{1}$ phase with the increase of x and this phenomenon is more obvious for $Li_{1.5}Ni_{0.13}Te_{0.37}O_2$ ($x=0.50$).

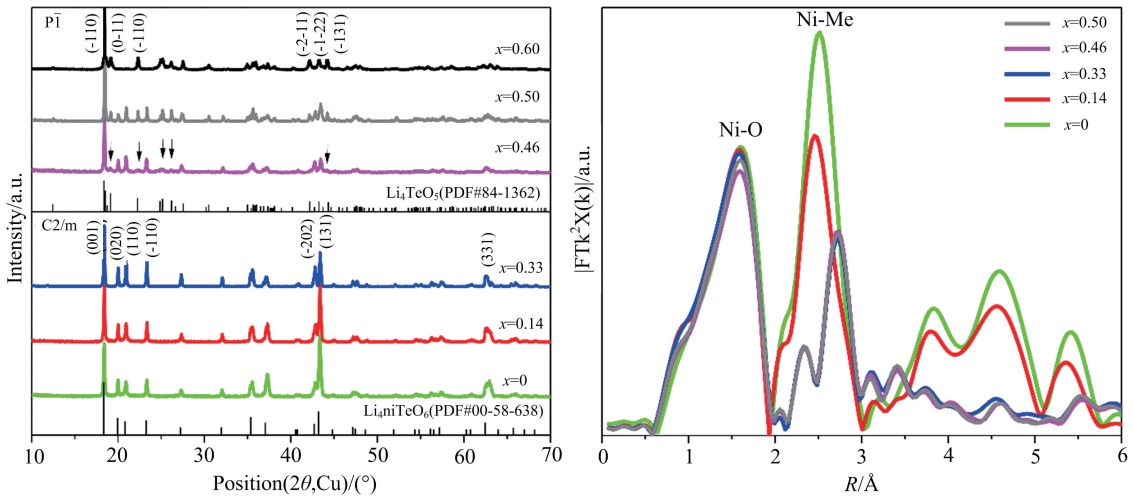

(a) XRD data　(b) Fourier transform EXAFS spectra

Fig. 1　Crystal/ atomic structural characterization of Li-Ni-Te-O materials

XRD characterizes long-range order in the crystal, while extended X-ray absorption fine structure (EXAFS) is related to the local atomic arrangement around the absorbed metal atom. Fig. 1(b) shows the EXAFS spectra of the as-prepared series samples. The first peak at around 1.5 Å (no phase correction) corresponds to the Ni-O bond as the first coordination sphere. The almost identical Ni-O pair indicates the oxygen distribution around Ni of these materials remained the same. The second peak at around 2.5 Å is related to the scattering contribution from the second neighboring Me (Me = Li, Ni or Te). Dramatic change can be observed for the Ni-Me pair, both by the intensity and the position. The intensity of the Ni-Me peak for $x=0$, 0.14 and 0.33 gradually decreases followed by a constant intensity for $x=0.46$ and $x=0.50$. It suggests that either the number of the metal coordinators reduces or the type of the coordinated metal atoms varies. For example, more lithium ions coordinate to the absorber Ni, replacing the other metal ions Ni or Te, because lithium of low-z atom contributes less scattering amplitude than metals of Ni and Te. The Ni-Me position shifts to the larger R direction for $x=0.33$, 0.46 and 0.50, indicating a larger distance between Ni and the second neighboring metal atoms.

Tab. 1 Important interatomic distances in $P\bar{1}$ structure

Atomic parameters				
Atom 1	Symmetry 1	Atom 2	Symmetry 2	Distance/Å
Te1	x, y, z	Li4	$1-x, 1-y, 1-z$	2.930 5(46)
Te1	x, y, z	Li2	$-x, -y, -z$	2.984 2(22)
Te1	x, y, z	Li4	x, y, z	2.915 0(52)
Te1	x, y, z	Li4	$1-x, 1-y, -z$	2.875 9(55)
Te1	x, y, z	Li2	$-x, -y, 1-z$	2.999 5(17)
Te1	x, y, z	Te1	$-x, -y, -z$	3.132 8(32)
Li1	x, y, z	O3	$-1+x, -1+y, z$	2.135 5(33)
Li1	x, y, z	O2	$-1+x, y, z$	2.034 8(29)
Te1	x, y, z	O3	$1-x, 1-y, -z$	1.884 4(33)
Te1	x, y, z	O2	$1-x, -y, -z$	2.021 1(33)
Te1	x, y, z	O4	x, y, z	1.876 0(33)

Similar to the preceding XRD result, the samples have been divided into two phases, $C2/m$ for $x=0$, 0.14, 0.33 and $P\bar{1}$ for $x=0.46$, 0.50 and 0.60. These two crystal structures give almost identical Ni-O local configuration and different Ni-Me local interaction. The composite of $x=0.33$ presents the $P\bar{1}$-like domain around Ni ions, revealed by the combined characterization of XRD and Synchrotron-based XAS. The $P\bar{1}$ structural parameters is shown in Tab. 1, which is referenced to Untenecker et al[27]. The distance (d) between Ni and surrounding Me-ions for $x=0.33$ is 2.96 Å ($d_{0.33}=2.96$ Å), which is an average value calculated from Tab. 1. While the difference between the d for $C2/m$ and $P\bar{1}$ is 0.22 Å, which is obtained from the EXAFS diagram in terms of the horizontal axis. And d_0 for $x=0$ is smaller than that for $x=0.33$, therefore d_0 is 2.74 Å. As shown in Fig. 2, the $C2/m$ structure gives a larger Ni-Me interaction distance than the $P\bar{1}$ structure ($d_{0.33}=2.96$ Å *vs.* $d_0=2.74$ Å) by favoring Li for making Ni coordinate rather than Ni or Te. Research shows that the barrier for migration of lithium is related to the TM valence and the Li-TM distance in layered lithium metal oxides[28-29]. A larger Li-TM distance and lower TM valence around Li support a lower barrier. To illustrate this point in detail, electrochemical properties will be discussed later. Therefore, XRD and EXAFS confirm a consistent structures for the samples, except for $x=0.33$ which combines the long-range order of $C2/m$ and the local structure of $P\bar{1}$.

Fig. 3(a) presents cycle performance at 0.1C (1C = 173mA · g^{-1}). The initial capacity for $x=0.33$ is 150 mAh · g^{-1} and capacity retention of 94% in comparison with 93, 121, 64 and 37 mAh · g^{-1} with a retention of 84%, 70%, 74%, and 73% for $x=0$, 0.14, 0.46, 0.50, respectively, after 50 cycles. That is, $x=0.33$ exhibits superior reversible Li^+ extraction. Fig. 3(b) shows the electrochemical impedance spectroscopy (EIS) measurement of the cathode series. The semicircle of the curve represents the charge transfer

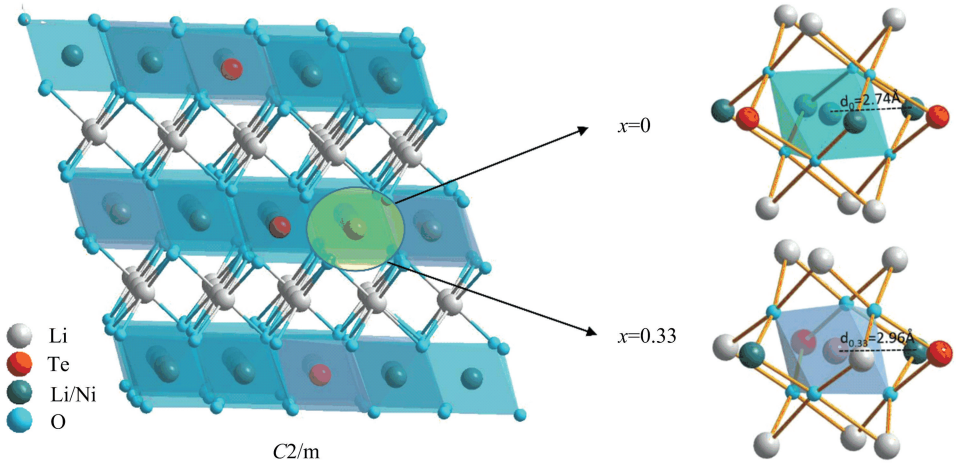

For $x=0.33$, the distance between Ni and surrounding Me-ions $d_{0.33}$ is 2.96 Å. While d_0 for $x=0$ is smaller than that of $x=0.33$, d_0 is 2.74 Å.

Fig. 2　Local structure models of Ni with $x=0$ and $x=0.33$

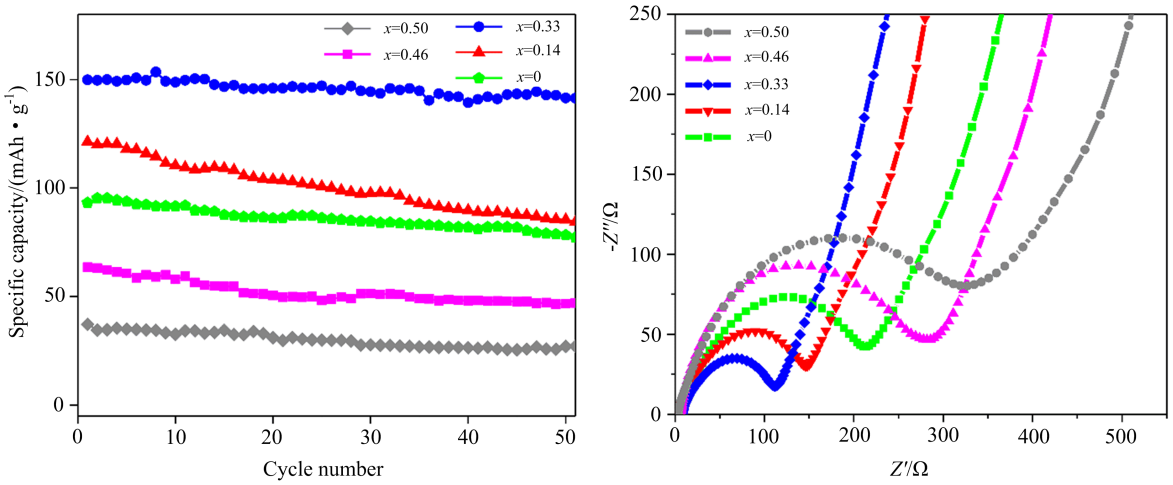

(a) Cycling performance at 0.1C　　(b) Electrochemical impedance plots

Fig. 3　Electrochemical properties of Li-Ni-Te-O

resistance at the interface of the electrolyte/electrode and the straight line is related to lithium diffusion resistance in the bulk of the electrode. It can be found that the diameter of the semicircle for $x=0.33$ is much smaller than that of the others, indicating that it has the lowest charge transfer resistance. The slope of the straight line for $x=0.33$ possesses the highest value, suggesting the fastest lithium diffusion. This result is in good agreement with the cycle performance. It is shown that $C2/m$ phase contributes towards high capacity but poor cycle performance, while $P\bar{1}$ phase exhibits low capacity but good cycle performance. Only $x=0.33$ with a $P\bar{1}$-like domain in the framework of $C2/m$ structure manifests both improved capacity and cycle performance. Previous research has shown that a larger Li-TM distance and lower TM valence around Li support more convenient Li^+ migration channels. Bao et al.[30] further investigated Li_4NiTeO_6 ($Li_{1.33}Ni_{0.33}Te_{0.33}O_2$, $x=0.33$) by focusing on the sequence of Li removal when it is charged through first-principles computations. Accordingly, $Li_{1.33}Ni_{0.33}Te_{0.33}O_2$ exhibits excellent electrical conductivity and structural stability with a volume change of 7.2%. Therefore, the loosely bonded structure for $x=0.33$ provides more convenient Li^+ migration channels, which leads to higher Li^+ mobility, as well as maintenance of structure stability.

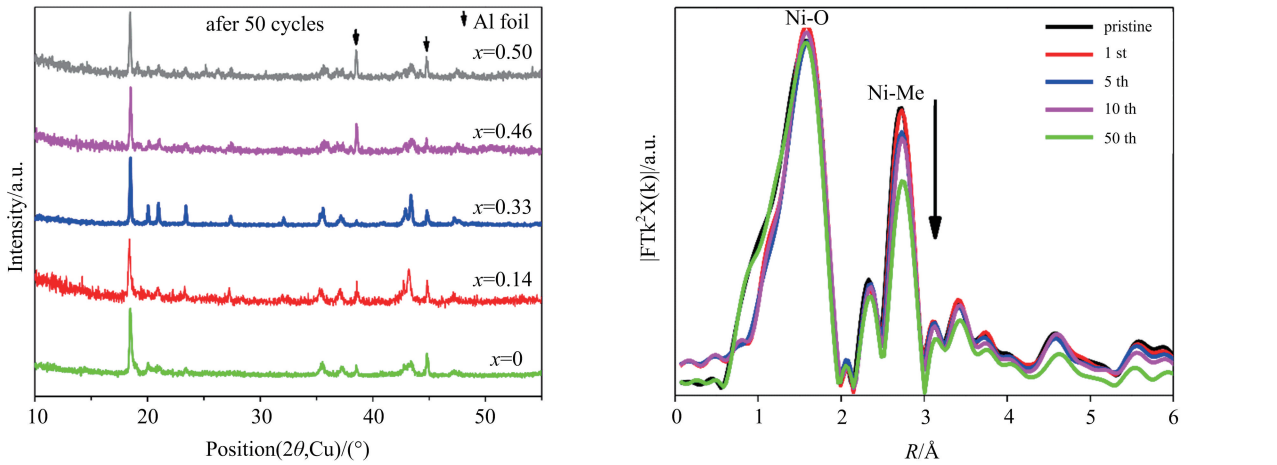

(a) XRD data after 50 cycles

(b) Ex situ FT-EXAFS curves for x=0.33 after the 1st, 5th, 10th and 50th cycle

Fig. 4 Evaluation of structural stability for Li-Ni-Te-O

Fig. 4(a) shows the XRD patterns after 50 cycles. For these samples, with the exception of $x=0.33$, the superlattice peaks within the range of 20° ~ 23° were broadened and weakened significantly, meaning a loss of the long-range stacking order. The XRD patterns for $x=0.33$ are consistent with the pristine phase, indicating a good structural stability. The Ni-Me local interaction for $x=0.33$ after cycling was checked by FT-EXAFS (Fig. 4(b)). The overall shapes are similar to each other, demonstrating an identical and stable local structure around Ni[31]. The most significant change is the slightly decreased peak intensity of the second shell that is attributed to the Me disorder around Ni. Hence, the steady patterns indicated by *ex situ* XRD and EXAFS means $x=0.33$ maintains a perfect structural stability even after 50 cycles.

The reversibility of the electrochemical process was tested by *ex situ* XPS and XANES measurement. XPS spectroscopy for $x=0.33$ was employed to obtain a deeper insight into the chemical valence states of the Ni and Te (Fig. 5(a)). Ni-2p core spectrum peak at 858.7 eV with a satellite peak at 864.5 eV reveals the existence of Ni^{2+} in the pristine phase[32]. Upon charge, Ni-$2p_{3/2}$ shifts to a higher binding energy of 860.0 eV, meaning a transformation of $Ni^{2+} \rightarrow Ni^{4+}$. After discharge, Ni-$2p_{3/2}$ binding energy shifts back to the pristine state, confirming that Ni^{4+} was reduced to Ni^{2+}. Even after 100 cycles, Ni-$2p_{3/2}$ is still similar to that of the discharge state, exhibiting good reversibility. Te-$3d_{5/2}$ spectrum gives a dominant peak at around 576.3 eV, which is characteristic of Te^{6+}[25]. Upon charge, this peak shows a shift to binding energy of 577.0 eV and an increase of the full width at half maximum (FWHM) value, which are reversed upon discharge. As is well known, tellurium is clearly without valence state higher than + 6. This phenomenon can be considered as a significant variation in the local environment around Te atom as mentioned by McCalla et al.[23]. XPS provides the valence state of the sample surface, while the synchrotron-based *ex situ* XANES measurement reveals the bulk information on the electronic state of atoms. In Fig. 5(b), Ni K-edge shifts to higher energy during the 1st charge process, indicating the continuous oxidation of Ni^{2+} to Ni^{4+}, which shifts back to low energy when discharged to 3.5 V. This trend is more prominent in the 2nd cycle (Fig. 5(c)).

Here we calculated the theoretical capacity for $x=0.33$ to be 172.9 mAh·g^{-1} considering Ni^{2+}/Ni^{4+} as the redox couple. Fig. 6(a) shows an initial discharge-capacity of 169.5 mAh·g^{-1} at 0.05C which is the highest capacity reported in Te-containing cathodes. The initial charge capacity of more than 250 mAh·g^{-1}, exceeding the theoretical limit, may derive from electrolyte

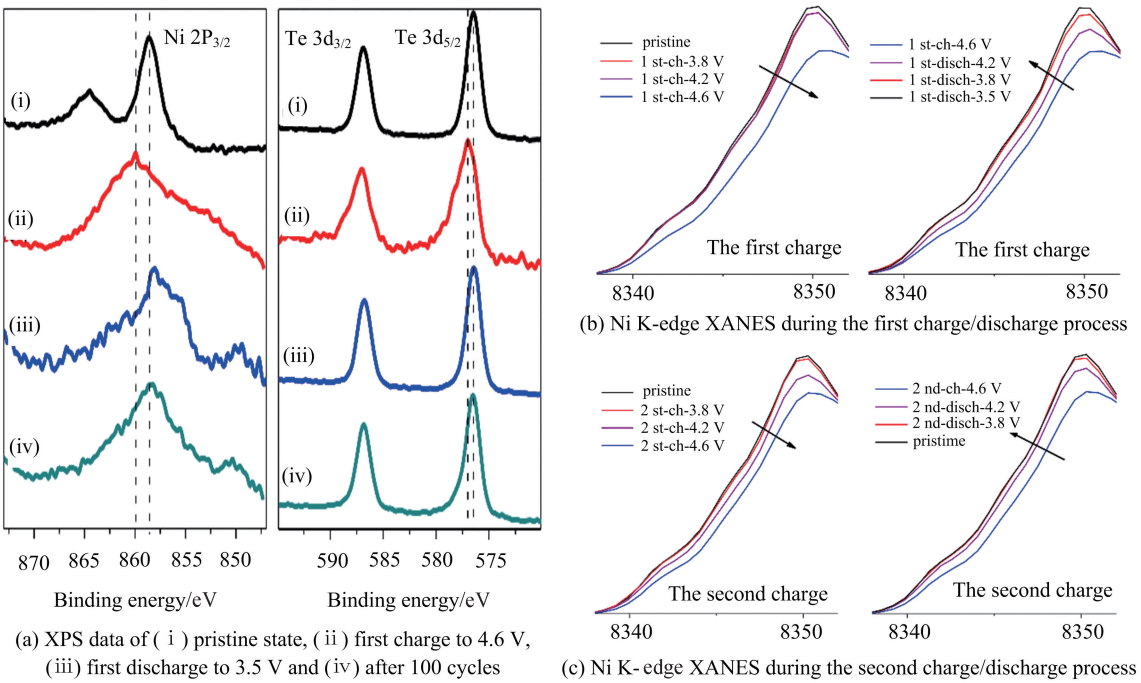

(a) XPS data of (ⅰ) pristine state, (ⅱ) first charge to 4.6 V, (ⅲ) first discharge to 3.5 V and (ⅳ) after 100 cycles

(b) Ni K-edge XANES during the first charge/discharge process

(c) Ni K-edge XANES during the second charge/discharge process

Fig. 5　Evaluation of electrochemical reversibility for $x=0.33$

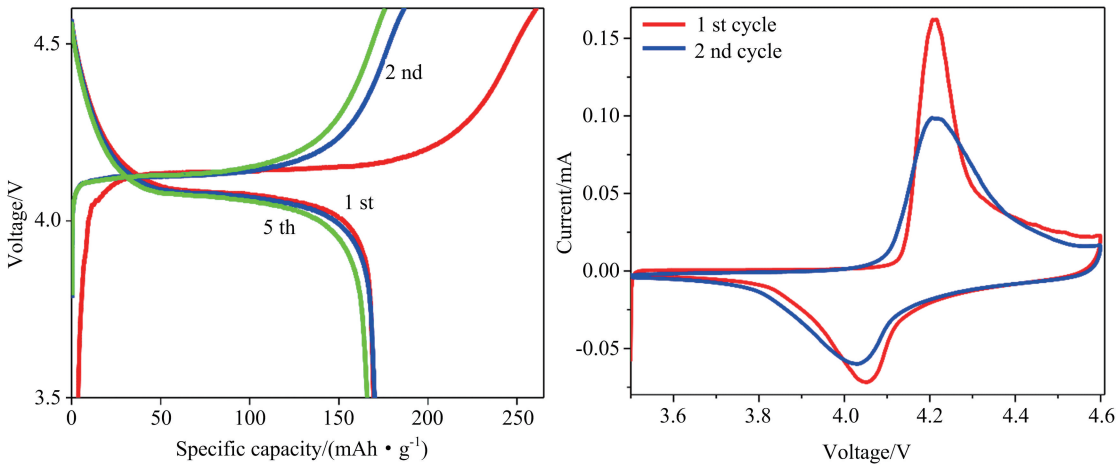

(a) Charge-discharge curves at 0.05C

(b) CV curves at a rate of 0.2 mV • s^{-1}

Fig. 6　Reconfirming electrochemical reversibility for $x=0.33$

decomposition, the O_2 generation caused by oxidization of O^{2-} or residual Li_2CO_3 decomposition[33-34]. The following charge capacity is around the theoretical value showing the irreversibility of capacity only exists in the first cycle. The CV curves (Fig. 6(b)) exhibited a pair of well-defined peaks, corresponding to the Ni^{2+}/Ni^{4+} redox couple. The position of redox peaks remained the same during the first two cycles, while only the intensities were changed, indicating that Ni^{2+}/Ni^{4+} was stable during the whole process. Based upon *ex situ* XPS, XANES, charge-discharge curves combined with CV results, an inference can be made confirming that the electrochemical reaction was sustained and stable.

3　Conclusion

In conclusion, a layered $Li_{1+x}Ni_{3/4-5/4x}Te_{1/4+1/4x}O_2$ cathode was synthesized and a unique $P\bar{1}$-like domain within the crystal framework of monoclinic $C2/m$ structure was found to improve the structural and electrochemical properties. This combined

structure makes $P\bar{1}$-like local domain providing a longer distance of the TM-TM interaction and then establishing a loosely bonded local structure, which contributes to higher Li^+ mobility, as well as maintaining the stability of the long-range order of $C2/m$. $Li_{1.33}Ni_{0.33}Te_{0.33}O_2$ exhibited excellent reversible Li^+ extraction with 94% capacity retention at 0.1C compared to other samples, with capacity retention of about 70% after 50 cycles. The synthesis of this stable crystal/atom structure would contribute significantly in developing high-performance cathodes.

References

[1] JANSE A N , KAHAIAN A J, KEPLE K D, et al. Development of a high-power lithium-ion battery [J]. Journal of Power Sources, 1999, 81: 902-905.

[2] SMITH K, WANG C Y. Power and thermal characterization of a lithium-ion battery pack for hybrid-electric vehicles [J]. Journal of Power Sources, 2006, 160(1): 662-673.

[3] ARMAND M, TARASCON J M. Building better batteries [J]. Nature, 2008, 451(7179): 652-657.

[4] THACKERAY M M, WOLVERTON C, ISAACS E D. Electrical energy storage for transportation-approaching the limits of, and going beyond, lithium-ion batteries [J]. Energy & Environmental Science, 2012, 5(7): 7854-7863.

[5] MIZUSHIMA K, JONES P C, WISEMAN P J, et al. Li_xCoO_2 ($0<x\leqslant 1$) : A new cathode material for batteries of high-energy density [J]. Solid State Ionics, 1981, 3-4: 171-174.

[6] OHZUKU T, UEDA A, NAGAYAMA M, et al. Comparative-study of $LiCoO_2$, $LiNi_{1/2}Co_{1/2}O_2$ and $LiNiO_2$ for 4-volt secondary lithium cells [J]. Electrochim Acta, 1993, 38(9): 1159-1167.

[7] KOKSBANG R, BARKER J, SHI H, et al. Cathode materials for lithium rocking chair batteries [J]. Solid State Ionics, 1996, 84(1/2): 1-21.

[8] LU X, SUN Y, JIAN Z L, et al. New insight into the atomic structure of electrochemically delithiated O3-$Li_{1-x}CoO_2$ ($0\leqslant x\leqslant 0.5$) nanoparticles [J]. Nano Letters, 2012, 12(12): 6192-6197.

[9] LIU W, OH P, LIU X, et al. Nickel-rich layered lithium transition-metal oxide for high-energy lithium-ion batteries [J]. Angew Chem Int Ed, 2015, 54(15): 4440-4457.

[10] OHZUKU T, MAKIMURA Y. Layered lithium insertion material of $LiNi_{1/2}Mn_{1/2}O_2$: A possible alternative to $LiCoO_2$ for advanced lithium-ion batteries [J]. Chemistry Letters, 2001, 8: 744-745.

[11] YOON W S, GREY C P, BALASUBRAMANIAN M, et al. In situ X-ray absorption spectroscopic study on $LiNi_{0.5}Mn_{0.5}O_2$ cathode material during electrochemical cycling [J]. Chemistry of Materials, 2003, 15(16): 3161-3169.

[12] YABUUCHI N, OHZUKU T. Novel lithium insertion material of $LiCo_{1/3}Ni_{1/3}Mn_{1/3}O_2$ for advanced lithium-ion batteries [J]. Journal of Power Sources, 2003, 119: 171-174.

[13] XU J, LIN F, NORDLUND D, et al. Elucidation of the surface characteristics and electrochemistry of high-performance $LiNiO_2$ [J]. Chemical Communications, 2016, 52(22): 4239-4242.

[14] DELMAS C, PERES J P, ROUGIER A, et al. On the behavior of the Li_xNiO_2 system: An electrochemical and structural overview [J]. Journal of Power Sources, 1997, 68(1): 120-125.

[15] SHIN D, WOLVERTON C, CROY J, et al. First-principles calculations, electrochemical and X-ray absorption studies of Li-Ni-PO_4 surface-treated $xLi_2MnO_3\cdot(1-x)LiMO_2$ (M = Mn, Ni, Co) electrodes for Li-ion batteries [J]. Journal of The Electrochemical Society, 2011, 159(2): A121-A127.

[16] SUN Y K, CHEN Z H, NOH H J, et al. Nanostructured high-energy cathode materials for advanced lithium batteries [J]. Nature Materials, 2012, 11(11): 942-947.

[17] MA X H, KANG K S, CEDER G, et al. Synthesis and electrochemical properties of layered $LiNi_{2/3}Sb_{1/3}O_2$ [J]. Journal of Power Sources, 2007, 173(1): 550-555.

[18] YABUUCHI N, TAHARA Y, KOMABA S, et al. Synthesis and electrochemical properties of Li_4MoO_5-NiO binary system as positive electrode materials for rechargeable lithium batteries [J]. Chemistry Of Materials, 2016, 28(2): 416-419.

[19] LAHA S, NATARAJAN S, GOPALAKRISHNAN J, et al. Oxygen-participated electrochemistry of new lithium-rich layered oxides Li_3MRuO_5 (M = Mn, Fe) [J]. Physical Chemistry Chemical Physics, 2015, 17(5): 3749-3760.

[20] MORET J, DANIEL F, LOEKSMANTO W, et al. Structure cristalline d'un oxotellurate, $Li_4Te^{VI}O_5$, à groupement anionique individualisé: $Te_2{}^{VI}O_{10}{}^{8-}$ [J]. Acta Crystallographica Section B, 1978, 34(11): 3156-3160.

[21] HEYMANN G, SELB E, KOGLER M, et al.

$Li_3Co_{1.06(1)}TeO_6$: Synthesis, single-crystal structure and physical properties of a new tellurate compound with Co^{II}/Co^{III} mixed valence and orthogonally oriented Li-ion channels [J]. Dalton Transactions, 2017, 46 (37): 12663-12674.

[22] GUPTA A, KUMAR V, UMA S. Interesting cationic ($Li^+/Fe^{3+}/Te^{6+}$) variations in new rocksalt ordered structures [J]. Journal of Chemical Sciences, 2015, 127(2): 225-233.

[23] MCCALLA E, PRAKASH A S, BERG E, et al. Reversible Li-intercalation through oxygen reactivity in Li-rich Li-Fe-Te oxide materials [J]. Journal of the Electrochemical Society, 2015, 162 (7): A1341-A1351.

[24] ZVEREVA E A, NALBANDYAN V B, EVSTIGNEEVA M A, et al. Magnetic and electrode properties, structure and phase relations of the layered triangular-lattice tellurate Li_4NiTeO_6 [J]. Journal of Solid State Chemistry, 2015, 225: 89-96.

[25] SATHIYA M, RAMESHA K, ROUSSE G, et al. Li_4NiTeO_6 as a positive electrode for Li-ion batteries [J]. Chemical Communications, 2013, 49 (97): 11376-11378.

[26] ARUNKUMAR P, JEONG W J, WON S, et al. Improved electrochemical reversibility of over-lithiated layered Li_2RuO_3 cathodes: Understanding aliovalent Co^{3+} substitution with excess lithium [J]. Journal of Power Sources, 2016, 324: 428-438.

[27] UNTENECKER H, HOPPE R. Ein neues oxotellurat, Na_4TeO_5, und eine revision der struktur von Li_4TeO_5 [J]. Journal of the Less Common Metals, 1987, 132(1): 79-92.

[28] KANG K, CEDER G. Factors that affect Li mobility in layered lithium transition metal oxides [J]. Physical Review B, 2006, 74(9): 094105.

[29] URBAN A, LEE J, CEDER G. The configurational space of rocksalt-type oxides for high-capacity lithium battery electrodes [J]. Advanced Energy Materials, 2014, 4(13): 13072-13072.

[30] BAO J, WU D, TANG Q, et al. First-principles investigations on delithiation of Li_4NiTeO_6 [J]. Physical Chemistry Chemical Physics, 2014, 16(30): 16145-16149.

[31] HUANG W, TAO S, ZHOU J, et al. Phase separations in $LiFe_{1-x}Mn_xPO_4$: A random stack model for efficient cathode materials [J]. The Journal of Physical Chemistry C, 2013, 118(2): 796-803.

[32] YABUUCHI N, LU Y C, MANSOUR A N, et al. The influence of heat-treatment temperature on the cation distribution of $LiNi_{0.5}Mn_{0.5}O_2$ and its rate capability in lithium rechargeable batteries [J]. Journal of The Electrochemical Society, 2011, 158 (2): A192-A200.

[33] YABUUCHI N, YOSHII K, MYUNG S T, et al. Detailed studies of a high-capacity electrode material for rechargeable batteries, Li_2MnO_3—$LiCo_{1/3}Ni_{1/3}Mn_{1/3}O_2$ [J]. Journal of the American Chemical Society, 2011, 133(12): 4404-4419.

[34] HONG J, LIM H D, LEE M, et al. Critical role of oxygen evolved from layered Li-excess metal oxides in lithium rechargeable batteries [J]. Chemistry of Materials, 2012, 24(14): 2692-2697.